Electronic Supplementary Material (ESI) for ChemComm.
This journal is © The Royal Society of Chemistry 2019

Electronic Supplementary Information for: Probing the existence of uranyl trisulfate structures in the AMEX solvent extraction process

Tamir Sukhbaatar,[a] Magali Duvail,[a] Thomas Dumas,[b] Sandrine Dourdain,*[a] Guilhem Arrachart,[a] Pier Lorenzo Solari,[c] Philippe Guilbaud [b] and Stéphane Pellet-Rostaing [a]

S1 Experimental

S1.1 Sample preparation

The organic phase was prepared by contacting an organic solution of 1 mol L^{-1} of tri-n-octylamine (TOA) and 3 % of octan-1-ol in *n*-dodecane, to an aqueous phase containing 10 mmol L^{-1} of uranium, 1 mol L^{-1} of H_2SO_4, and 1 mol L^{-1} of Li_2SO_4. Extractions were performed at room temperature by contacting and mixing 1/1 volumes of aqueous and organic phases during 1 hour in a mixer at 400 rpm. The organic phase was further separated after a centrifugation stage at 4000 rpm for 30 minutes.

S1.2 Extraction analysis

Uranium extraction was analysed by Inductively Coupled Plasma Atomic Emission Spectrophotometry (ICP-AES, Spectro Arcos). The content in the organic phase was deduced by difference method by measuring the aqueous phase before and after extraction. Water extraction was characterized by Karl Fisher titration of the organic phases using a Metrohm 831 KF Coulometer, and sulfuric acid extraction was determined by pH titration of the organic phase.

Composition of the organic phase after extraction is given in Table S1.

Table S1 Composition of the organic phase after extraction[(a)]

TOA	Octanol	UO_2^{2+}	H_2O	H^+
100	190[(b)]	7.3	4.6	220

[(a)] Concentrations are given in mmol L^{-1}.

It can be noticed that less than 1 water molecule is transferred to the organic phase. Considering the possible extraction/solubilisation of water by octan-1-ol dimers or by the TOA/octan-1-ol aggregates that do not complexe any uranium, it is reasonable to consider that no water molecule intervenes in the first coordination sphere for the complexed uranium.

[a] *ICSM, CEA, CNRS, ENSCM, Univ Montpellier, Marcoule, France. Fax: +33 (0)4 66 79 76 11; Tel: +33 (0)4 66 33 93 09; E-mail: sandrine.dourdain@cea.fr*
[b] *CEA, DEN, MAR, DMRC, SPDS, LILA, F-30207 Bagnols-sur-Cèze Cedex, France.*
[c] *Synchrotron SOLEIL, L'Orme des Merisiers, Saint-Aubin – BP 48, 91192 Gif-sur-Yvette Cedex, France.*

S1.3 Effect of water and/or octan-1-ol molecules on the EXAFS spectra fit

To estimate the effect of hypothetical coordinating water and/or octan-1-ol molecules on the EXAFS fit, the fit model was implemented with a third O atom shell in the uranyl equatorial coordination sphere. The experimental spectra fit is performed again with a varying number of water and/or octan-1-ol molecules (0 to 2). The resulting fits are presented in Figure S1.

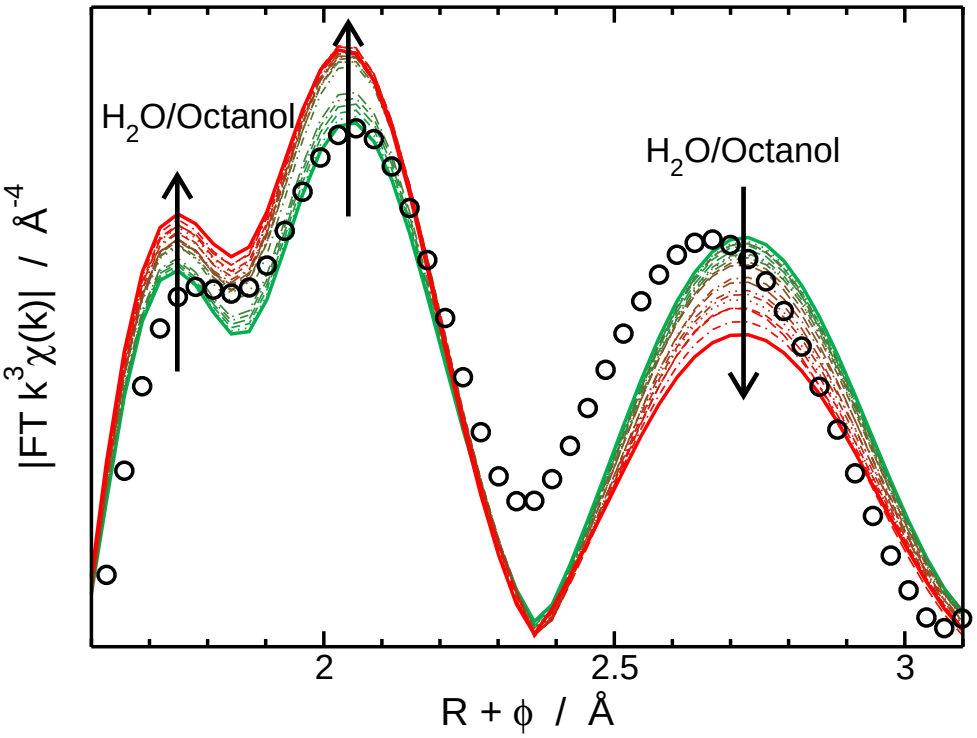

Fig. S1 Fit of the experimental oxygen and sulfur EXAFS signal with a varying number of water and/or octan-1-ol molecules in the uranyl coordination sphere (green full line is 0 octan-1-ol and/or water molecule, red full is 2, intermediates values are in dotted lines).

It shows a decrease in the fit agreement with the increasing number of water and/or octan-1-ol molecules: from 0 (green full line) to 2 (red full line). In detail, the increase in the water and/or octan-1-ol coordination trend to increase the EXAFS signal for the equatorial oxygen donor atoms $1.6 < R + \phi < 2.4$. This effect is spuriously balanced in the fit by a concomitant decrease in the number of coordinating sulfate group (since the coordination numbers for $O_{mono/bi}$ and $S_{mono/bi}$ are related coordinated numbers). Hence, as the octan-1-ol and/or water molecules are included poorer agreement in the sulfur atoms coordination shell $2.4 < R + \phi < 3.1$ are observed. Overall, considering the very intense sulfur atom contribution in the experimental spectra, the best agreement is obtain with only sulfate ligand in the first coordination shell. Any other configuration results in either, a poor spectral agreement, or to a total number of equatorial oxygen atoms higher than six, associated with irrevelent DWF values (typically larger than 10^{-2} Å^2).

S2 EXAFS data acquisition and treatments

X-ray absorption spectra were recorded at MARS beamline of SOLEIL Synchrotron. The monochromator energy scale was calibrated to the K-edge of a Yttrium metal foil. The spectra were recorded at the Uranium L_{III}-edge (17185 eV) in fluorescence mode and the results were processed using Athena and Artemis softwares[1]. Scattering paths and amplitudes were calculated by using FEFF 8.4[2] from two selected structures issued from the molecular dynamic model. Data were fitted in *R*-space between 1 and 4 Å after $k^3\chi(k)$ Fourier transform between 3 and 14.5 $Å^{-1}$.

S3 MD simulations

S3.1 Simulation details

Here, one complex composed on one UO_2^{2+} cation, three SO_4^{2-} anions, four TOA molecules in 719 *n*-dodecane molecules have been simulated by means of molecular dynamics simulations using explicit polarization. Simulations have been carried out with SANDER14, a module of AMBER14[3] using explicit polarization in the NPT ensemble. Periodic boundary conditions were applied to the simulation box. Long-range interactions have been calculated using the particle-mesh Ewald method[4]. Equations of motion were numerically integrated using a 1 fs time step. Systems were previously equilibrated at room temperature (298.15 K) over at least 300 ps, and production runs were subsequently collected for 15 ns. For the simulations, experimental isothermal compressibility of *n*-dodecane[5,6] (κ = 9.9×10^{-10} m s^2 kg^{-1} = 98.8×10^6 bar^{-1}) has been used.

S3.1.1 UO_2^{2+}

The force field used for describing the UO_2^{2+} cation is the one recently developed[7]. It allows for calculating structural properties of UO_2^{2+} in good agreement with the experiments in both aqueous and organic (with DMDOHEMA molecules in *n*-heptane) phases. The force field parameters are given in Table S2.

Table S2 Parameters used for describing UO_2^{2+} in aqueous solutions by molecular dynamics simulations using explicit polarization

Atom	ε^a	σ^b	q^c	α^d
$U_{UO_2^{2+}}$	0.112	3.332	+2.30	0.720
$O_{UO_2^{2+}}$	1.795	2.835	-0.15	0.156

bond	$R_0{}^b$	$K_R{}^e$
$U_{UO_2^{2+}} - O_{yl}$	1.75	1255.2

[a] Energy (in kJ mol^{-1}). [b] Distance (in Å). [c] Partial atomic charge (in *e*). [d] Atomic polarizability (in $Å^3$). [e] Bending constant (in kJ mol^{-1} $Å^{-2}$).

S3.1.2 SO_4^{2-}

The force field used for describing the SO_4^{2-} anion is the one originally developed in Ref.[8]. However, it should be noted here that the partial atomic charges used for SO_4^{2-} are the ones calculated using the RESP method without rescaling to take into account the polarization since SO_4^{2-} has no dipole. Therefore, we used q_S = +1.3282 e, and q_O = -0.83205 e. Furthermore, the atomic polarizabilities on S and O determined by van Duijnen *et al.* have been used[9]. The Lennard-Jones (LJ) parameters remain the same as in Ref.[8].

S3.1.3 *n*-dodecane

The force field used for describing the *n*-dodecane molecule, and more precisely the LJ parameters, has slightly been modified compared to the one used for describing the *n*-heptane[10]. Indeed, atomic polarizabilities have been modified with respect to the ones determined from *ab initio* calculations by van Duijnen *et al.*[9]. Here, it should be noted that only the atomic polarizability of the carbon atom has been modified (atomic polarizability of H is the same as the one defined in the parm99 AMBER force field[11]). Furthermore, LJ parameters have also been modified. Indeed, instead of using the parm99 ones, that are the OPLS[12] ones, we used those determined by Siu *et al.* for long hydrocarbon chains[13]. Indeed, because of crystallization phenomenon generally observed from MD simulations for long aliphatic chains, and therefore for *n*-dodecane, LJ parameters on the H atoms have been modified that allows for describing correctly both small and long aliphatic chains (Tab. S3).

Table S3 Parameters used for describing the *n*-dodecane molecule by molecular dynamics simulations using explicit polarization

Atom	ε^a	σ^b	α^c	Ref.
CT	0.276	3.5000	0.482	Siu *et al.*[13]
HC	0.126	2.5000	0.135	Siu *et al.*[13]
CT	0.458	3.4000	0.878	Parm99[11]
HC	0.066	2.6500	0.135	Parm99[11]

[a] Energy (in kJ mol^{-1}). [b] Distance (in Å). [c] Atomic polarizability (in Å^3).

Partial atomic charges for the *n*-dodecane molecule have been determined from *ab initio* calculations with Gaussian09[14] using the RESP (Restricted Electrostatic Potential) procedure[15] (Fig. S2).

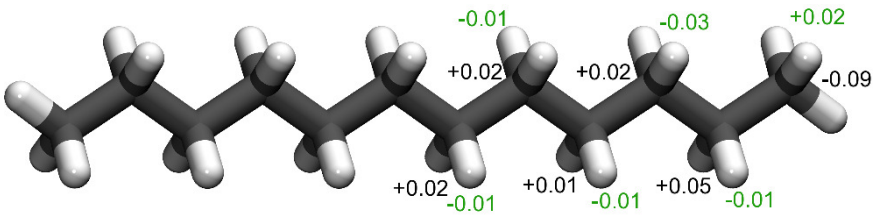

Fig. S2 Partial atomic charges for the *n*-dodecane molecule.

All these parameters allows for avoiding observing the well-known crystallization phenomenon generally observed from MD simulations for long aliphatic chains, typically for n-alkanes with $n \geq 8$ [13,16,17] (Fig. S3).

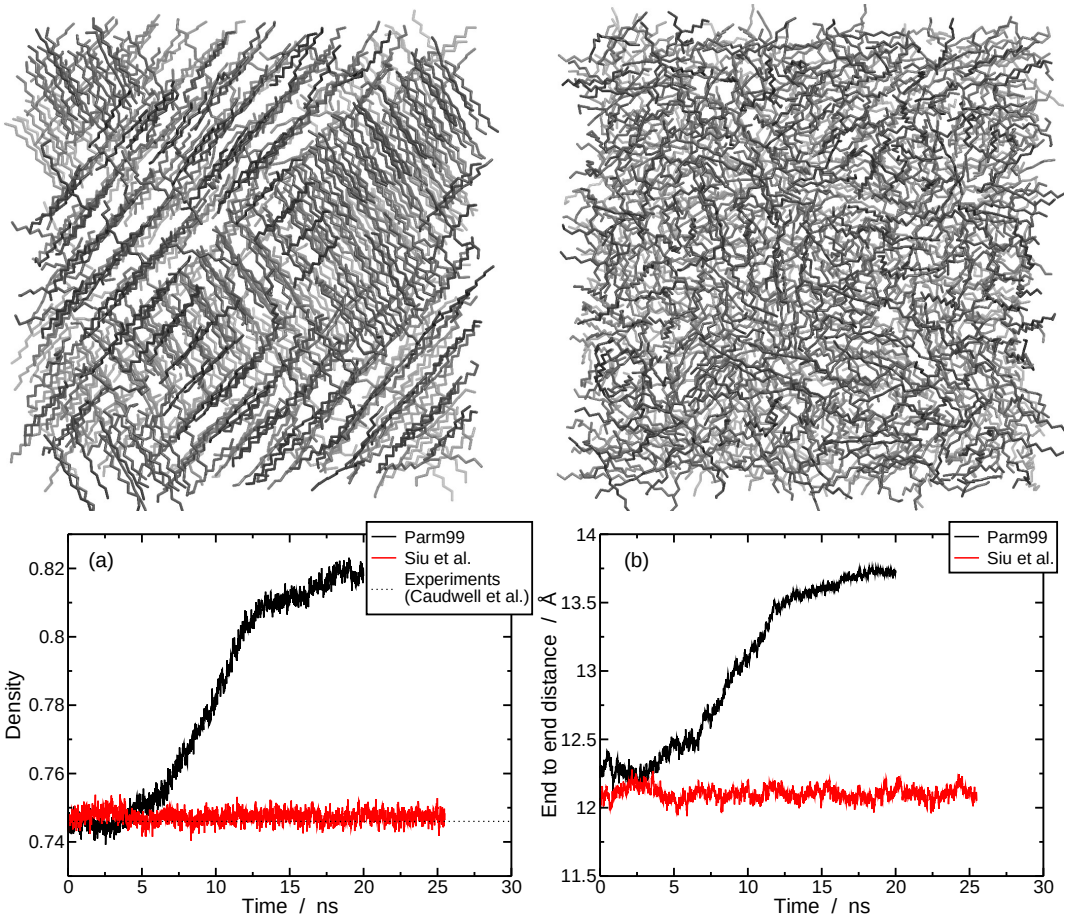

Fig. S3 (Top) Snapshots issued from MD representing 750 n-dodecane (left) and 1000 n-dodecane (right) simulation boxes calculated using the parm99 [11] (left) and Siu *et al.* [13] (right) force field parameters. (Bottom) Variation of the (a) densities and (b) the average length of the n-dodecane chain as a function of the simulation time calculated using the parm99 [11] (black) and Siu *et al.* [13] (red) force field parameters. Experimental density of n-dodecane (ρ_{exp} = 746 kg m^{-3}) is issued from Ref. [18]

Furthermore, the properties of the n-dodecane are in good agreement with the experiments, and more precisely the density $d_{\text{MD}} = 0.747 \pm 0.002$ *vs.* $d_{\text{exp}} = 0.746 \pm 0.001$ [18].

Note that using these parameters allows for using a cutoff value of 12 Å as well as 15 Å without any consequences on the density calculated, contrary to the use of the parm99 force field. Indeed, the crystallization phenomenon occurred as faster as the cutoff was high.

S3.1.4 TOA

Here, we consider that the tri-n-octylamine (TOA) molecule is protonated. LJ parameters used for the carbon and hydrogen atoms of the aliphatic chains of the TOA molecule are

the same the ones used for the *n*-dodecane. For the other atom types, i.e., the nitrogen and hydrogen atoms in the vicinity of the nitrogen atom, the parm99[11] force field parameters have been used. As already mentioned, atomic polarizabilities used here are the ones determined by van Duijnen *et al.*[9], except for the H atoms, and the partial atomic charges have been calculated using the RESP procedure. LJ parameters and partial atomic charges for the TOA are given in Table S4 and Figure S4.

Table S4 Parameters used for describing the TOA molecule by molecular dynamics simulations using explicit polarization

Atom	ε^a	σ^b	α^c	Ref.
N3	0.711	3.2500	0.276	Parm99[11]
CT	0.276	3.5000	0.482	Siu *et al.*[13]
HC	0.126	2.5000	0.135	Siu *et al.*[13]
H1	0.066	2.6500	0.135	Parm99[11]
H	0.066	1.0700	0.161	Parm99[11]

[a] Energy (in kJ mol^{-1}). [b] Distance (in Å). [c] Atomic polarizability (in Å^3).

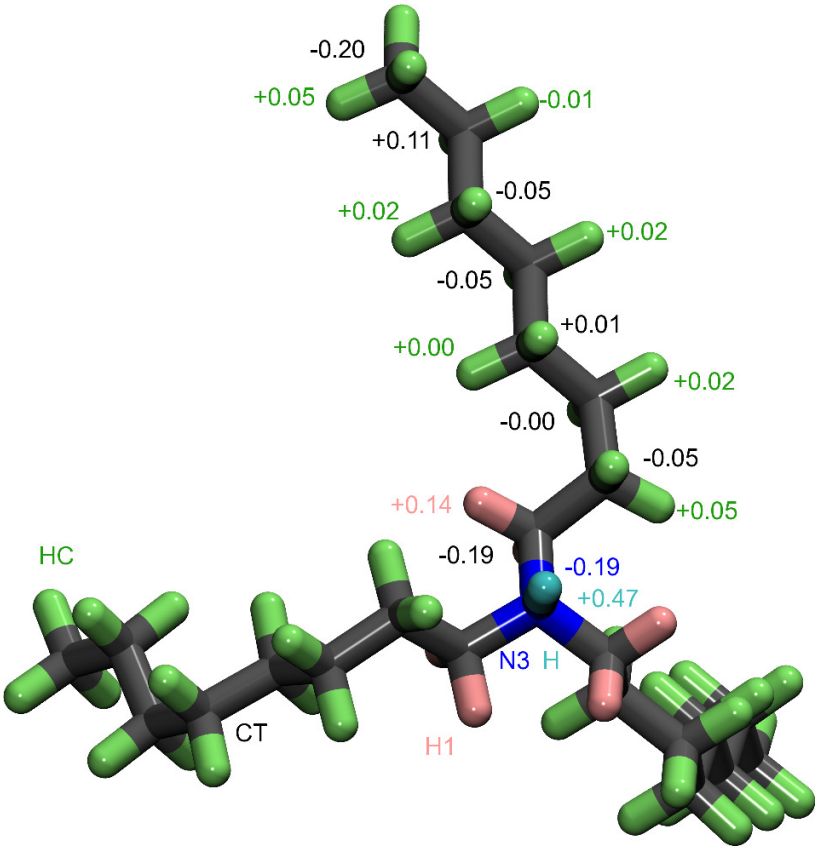

Fig. S4 Atom types and partial atomic charges of the TOA molecule. For clarity, partial atomic charges have been written in the same color as the atom type, i.e., H (cyan): H bonded to nitrogen atoms; CT (gray): sp3 aliphatic C; HC (green): H aliphatic bonded to C without electron-withdrawing group; H1 (pink): H aliphatic bonded to C with 1 electron-withdrawing group; N3 (blue): sp3 N for charged amino groups.

S3.2 EXAFS

Theoretical EXAFS signals have been calculated directly from snapshots issued from molecular dynamics simulations, typically each picosecond, using the FEFF8.4 program[2], and then analyzed by means of the IFFEFIT software[1].

S4 Figures

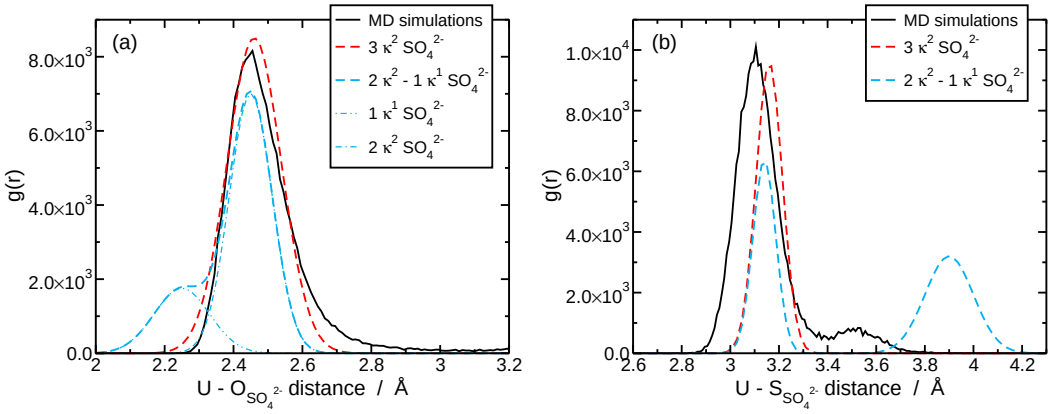

Fig. S5 Radial distribution functions (black solid line) calculated for (a) U – $O_{SO_4^{2-}}$, and (b) U – $S_{SO_4^{2-}}$. Theoretical radial distribution functions calculated from the experimental metrical parameters are also plotted (dashed line) for the 3 κ^2 SO_4^{2-} (red) and the 2 κ – 1 κ SO_4^{2-} (blue) configurations.

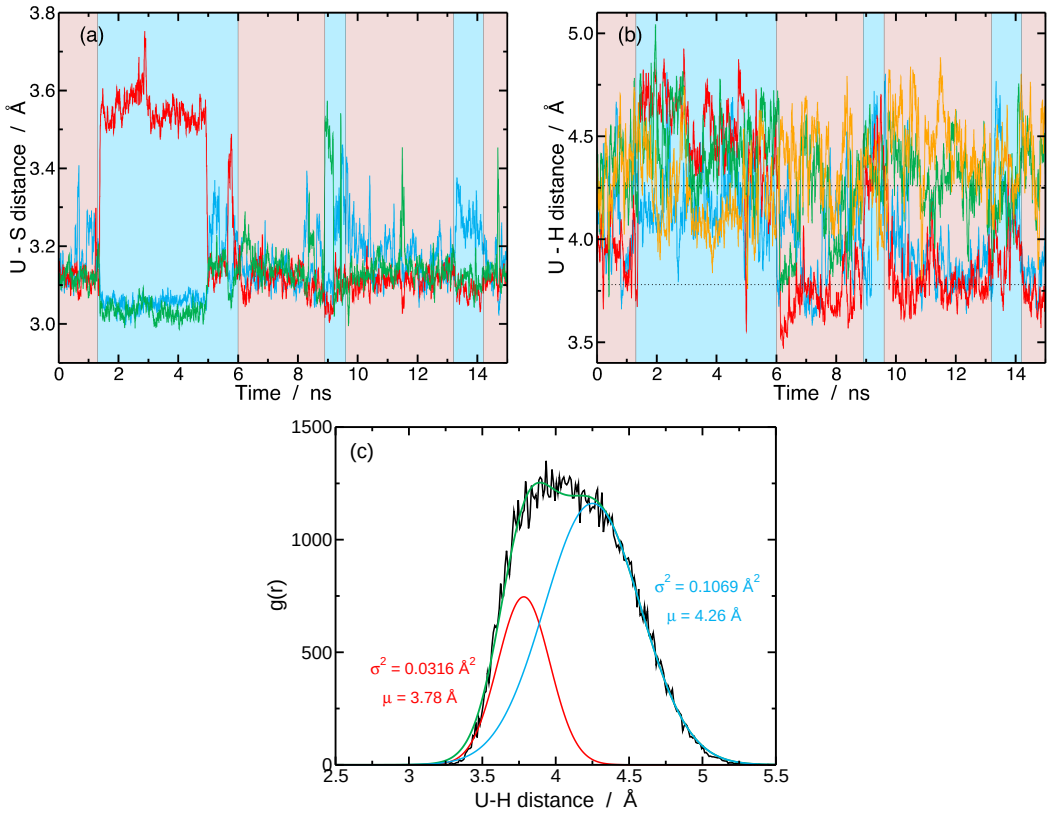

Fig. S6 (a) U – $S_{SO_4^{2-}}$ distances and (b) U – H_{TOA} distances calculated from MD simulation as a function of the simulation time. The blue backgroung corresponds to 2 κ^2 – 1 κ^1 configurations, and the red background corresponds to 3 κ^2 configurations. (c) U – H_{TOA} radial distribution function calculated for the corresponding simulation.

References

1 B. Ravel and M. Newville, *J. Synchrotron Rad.*, 2005, **12**, 537–541.

2 J. J. Rehr and R. C. Albers, *Rev. Mod. Phys.*, 2000, **72**, 621–654.

3 D. A. Case, V. Babin, J. T. Berryman, R. M. Betz, Q. Cai, D. S. Cerutti, T. E. Cheatham, III, T. A. Darden, R. E. Duke, H. Gohlke, A. W. Goetz, S. Gusarov, N. Homeyer, P. Janowski, J. Kaus, I. Kolossváry, A. Kovalenko, T. S. Lee, S. LeGrand, T. Luchko, R. Luo, B. Madej, K. M. Merz, F. Paesani, D. R. Roe, A. Roitberg, C. Sagui, R. Salomon-Ferrer, G. Seabra, C. L. Simmerling, W. Smith, J. Swails, R. C. Walker, J. Wang, R. M. Wolf, X. Wu and P. Kollman, *AMBER 14*, 2014, University of California, San Francisco.

4 T. Darden, D. York and L. Pedersen, *J. Chem. Phys.*, 1993, **98**, 10089–10092.

5 M. Diaz Peña, G. Tardajos, R. Arenosa and C. Menduiña, *J. Chem. Thermodyn.*, 1979, **11**, 951 – 957.

6 A. T. Balaban, N. H. March and D. J. Klein, *Phys. Chem. Liq.*, 2009, **47**, 1–4.

7 M. Duvail, T. Dumas, A. Paquet, A. Coste, L. Berthon and P. Guilbaud, *Phys. Chem. Chem. Phys.*, 2019, **accepted**,.

8 M. Duvail, A. Villard, T.-N. Nguyen and J.-F. Dufrêche, *J. Phys. Chem. B*, 2015, **119**, 11184–11195.

9 P. T. van Duijnen and M. Swart, *J. Phys. Chem. A*, 1998, **102**, 2399–2407.

10 Y. Chen, M. Duvail, P. Guilbaud and J.-F. Dufrêche, *Phys. Chem. Chem. Phys.*, 2017, **19**, 7094–7100.

11 D. A. Case, T. E. Cheatham, T. Darden, H. Gohlke, R. Luo, K. M. Merz, A. Onufriev, C. Simmerling, B. Wang and R. J. Woods, *J. Comput. Chem.*, 2005, **26**, 1668–1688.

12 W. L. Jorgensen, D. S. Maxwell and J. Tirado-Rives, *J. Am. Chem. Soc.*, 1996, **118**, 11225–11236.

13 S. W. I. Siu, K. Pluhackova and R. A. Böckmann, *J. Chem. Theory. Comp.*, 2012, **8**, 1459–1470.

14 M. J. Frisch, G. W. Trucks, H. B. Schlegel, G. E. Scuseria, M. A. Robb, J. R. Cheeseman, G. Scalmani, V. Barone, B. Mennucci, G. A. Petersson, H. Nakatsuji, M. Caricato, X. Li, H. P. Hratchian, A. F. Izmaylov, J. Bloino, G. Zheng, J. L. Sonnenberg, M. Hada, M. Ehara, K. Toyota, R. Fukuda, J. Hasegawa, M. Ishida, T. Nakajima, Y. Honda, O. Kitao, H. Nakai, T. Vreven, J. A. Montgomery, Jr., J. E. Peralta, F. Ogliaro, M. Bearpark, J. J. Heyd, E. Brothers, K. N. Kudin, V. N. Staroverov, R. Kobayashi, J. Normand, K. Raghavachari, A. Rendell, J. C. Burant, S. S. Iyengar, J. Tomasi, M. Cossi, N. Rega, J. M. Millam, M. Klene, J. E. Knox, J. B. Cross, V. Bakken, C. Adamo, J. Jaramillo, R. Gomperts, R. E. Stratmann, O. Yazyev, A. J. Austin, R. Cammi, C. Pomelli, J. W. Ochterski, R. L. Martin, K. Morokuma, V. G. Zakrzewski, G. A. Voth, P. Salvador, J. J. Dannenberg, S. Dapprich, A. D. Daniels, Ö. Farkas, J. B. Foresman, J. V. Ortiz, J. Cioslowski and D. J. Fox, *Gaussian 09 Revision D.01*, 2013, Gaussian Inc. Wallingford CT.

15 C. I. Bayly, P. Cieplak, W. Cornell and P. A. Kollman, *J. Phys. Chem.*, 1993, **97**, 10269–10280.

16 X. Ye, S. Cui, V. F. de Almeida and B. Khomami, *J. Mol. Model.*, 2013, **19**, 1251–1258.

17 R.-G. Xu, Y. Xiang and Y. Leng, *J. Chem. Phys.*, 2017, **147**, 054705.
18 D. R. Caudwell, J. P. M. Trusler, V. Vesovic and W. A. Wakeham, *Int. J. Thermophys.*, 2004, **25**, 1339–1352.